

Neutron Background Simulations for LEGEND-1000 in a Geant4-based Framework

CJ Barton, University of South Dakota
On behalf of the LEGEND Collaboration



31 July 2020

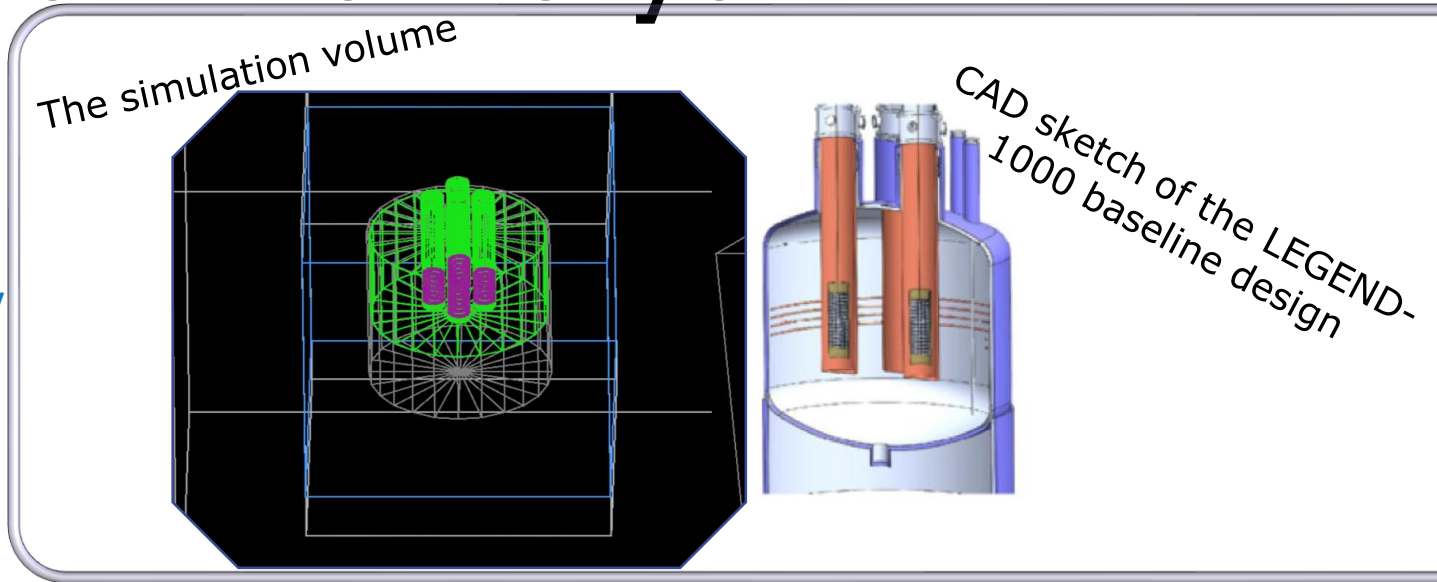
Max Planck Society (MPG)
European Research Council
Foundation for Polish Science
Polish National Science Centre (NCN)
Swiss National Science Foundation (SNF)
Russian Foundation for Basic Research (RFBR)
Italian Istituto Nazionale di Fisica Nucleare (INFN)
We thank our hosts and colleagues at LNGS and SURF

We appreciate the support of our sponsors:

We thank the ORNL Leadership Computing Facility and the LBNL NERSC Center
German Research Foundation (DFG), Excellence Cluster ORIGINS and SFB1258
Science and Technology Facilities Council, part of UK Research and Innovation
U.S. Department of Energy, Office of Nuclear Physics (DOE-NP)
Canada Foundation for Innovation, John R. Evans Leaders Fund
Research Council of Canada, Natural Sciences and Engineering
German Federal Ministry for Education and Research (BMBF)
U.S. National Science Foundation, Nuclear Physics (NSF)
U.S. Department of Energy, Through the LANL, ORNL & LBNL LDRD programs

LEGEND and Neutrons from cryostat wall

Mission statement : The LEGEND (Large Enriched Germanium Experiment for Neutrinoless $\beta\beta$ Decay) collaboration aims to develop a phased, **Ge-76 based** double-beta decay experimental program with discovery potential at a **half-life beyond 10^{28} years**, using existing resources as appropriate to expedite physics results.



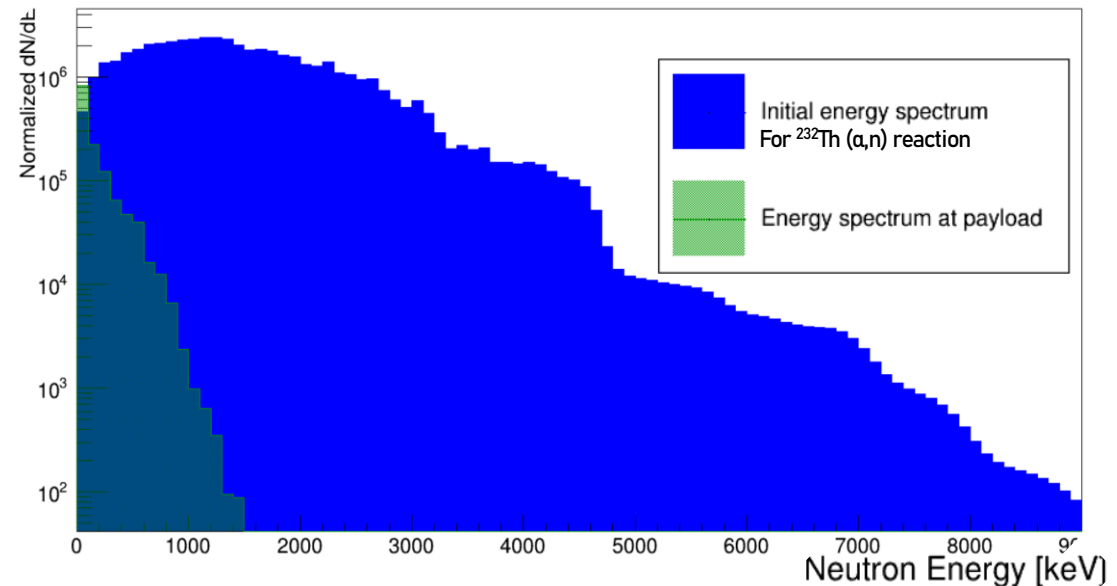
Dominant contributor of radiogenic neutrons

Created by fission and (α, n) reactions due to decay of heavy element impurities in the steel

Initial spectrum generated using NeoCBOT
S.Westerdale et al, NIMA 875 (2017) 57-64

GEANT4-based simulations suggest radiogenic neutron background subdominant to the cosmogenic neutron background

Normalized sampling spectrum and spectrum of neutrons reaching a payload



In-situ cosmogenic neutrons

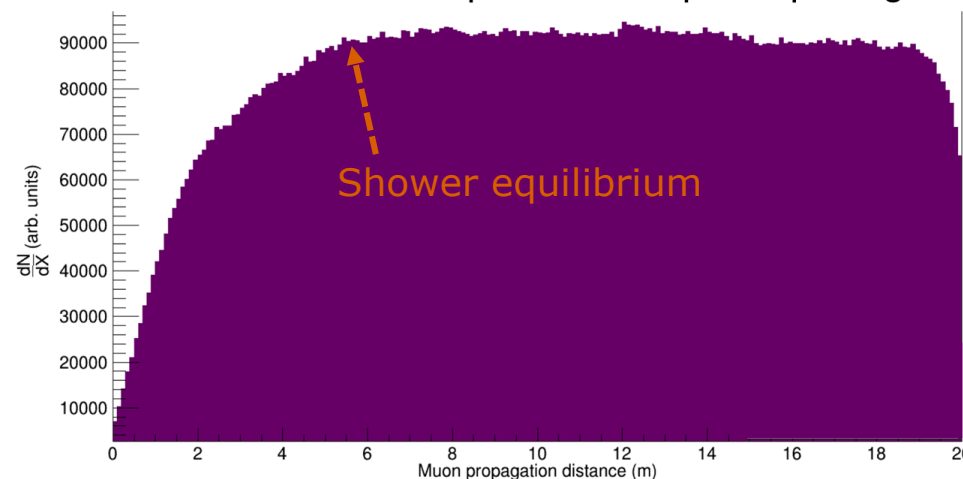
Primarily created in hadronic muon showers

Large shielding with high Z material may lead to significant cosmogenic backgrounds

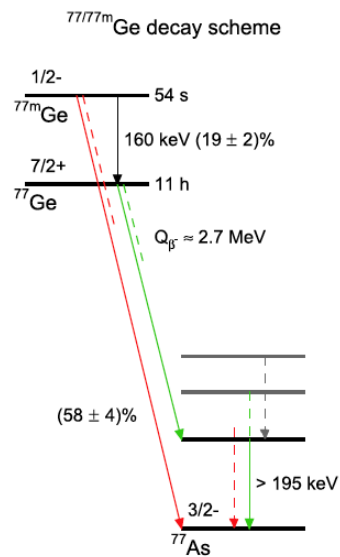
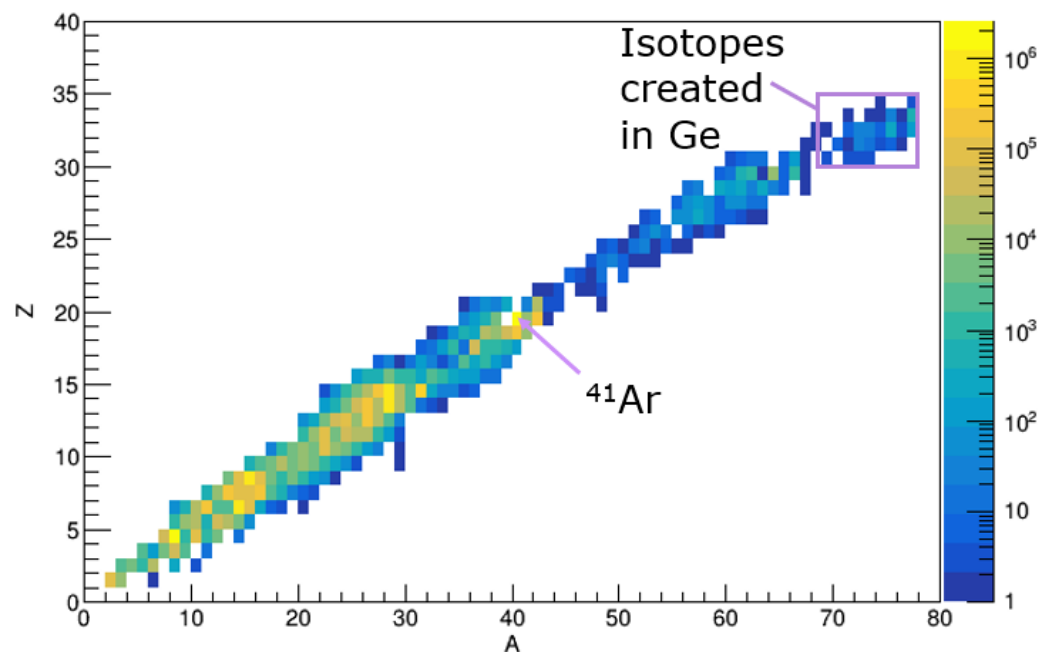
Complex shower development, largely dictated by muon path length and material

Shower development/isotope production investigated using Geant4 simulations

Muon-induced neutron production in pure liquid argon



A and Z numbers of nuclear isotopes generated (all materials)

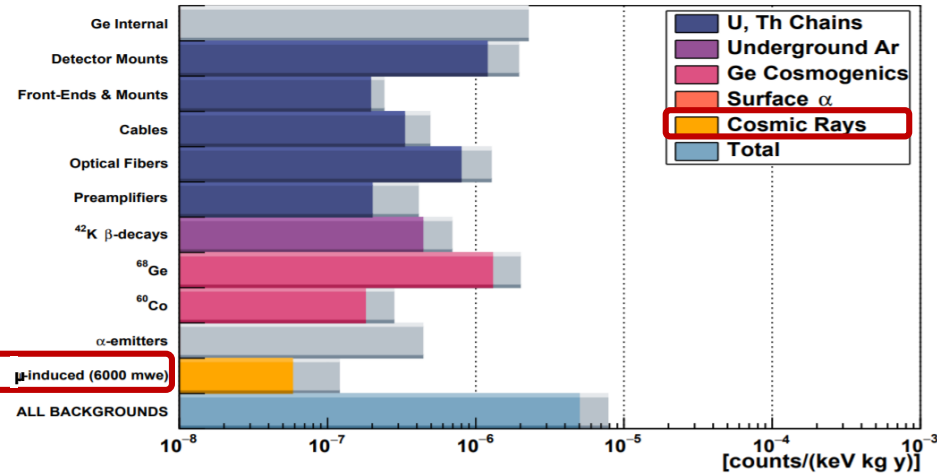


From Eur. Phys. J. C (2018) 78:597

Wide variety of isotopes generated by muon passage
Few isotopes can contribute to ^{76}Ge $0\nu\beta\beta$ background
Cosmogenic isotopes ^{77}Ge and $^{77\text{m}}\text{Ge}$ expected to contribute, based on decay energies and mean lifetime
Mitigated by shielding, active veto, and analysis cuts

Mitigation options for cosmogenic neutrons

Cosmogenic background highly dependent on host site for LEGEND-1000. SNOLAB depth assumed



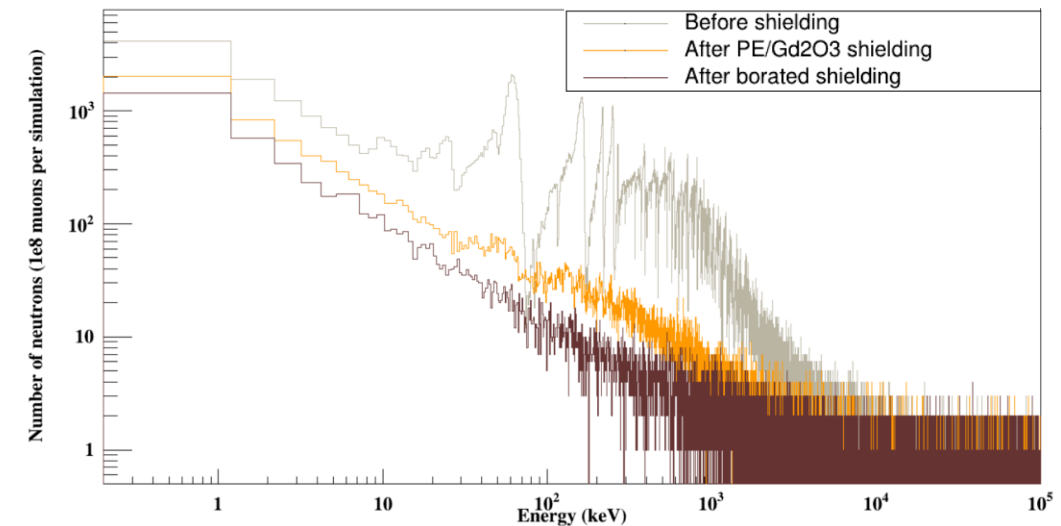
Polyethylene + neutron absorber

- 10 cm thick shields with outer radius 2m centered on detector array
- Polyethylene moderator, with gadolinium or boron to capture
- Both options significantly reduced neutron flux on detectors
 - ^{77}Ge and $^{77\text{m}}\text{Ge}$ production rate roughly halved in both cases
- Additional radiogenic neutrons, such as (α ,n) neutrons from borated PE impurities, reduce shielding effectiveness

Liquid argon doping

- Isotopes added to liquid argon surrounding detectors:
 - ^{131}Xe , in 100ppm and 1000 ppm quantities
 - ^3He , in 0.1% and 1% mass fraction
- No significant change in neutron flux for ^{131}Xe doping
 - New neutrons are created in other channels
- Initial results of ^3He study show reduced neutron flux
 - More expensive to implement in practice

Neutron energy spectra before and after shielding options



Cosmic and atmospheric background stability with (stopping) muons in the SoLid experiment

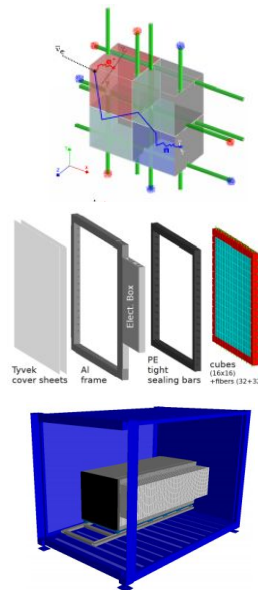
Giel Vandierendonck
on behalf of the SoLid collaboration



SoLid

Phase 1 detector

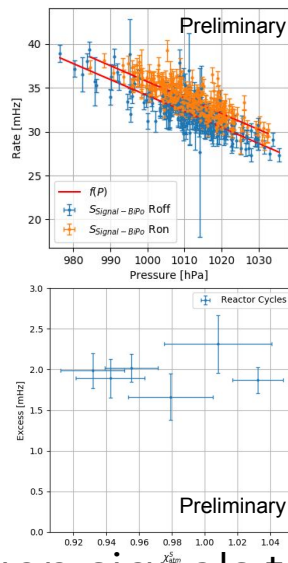
- 12800 Cubes
 - PVT → EMs ($e/\gamma/\mu$)
 - ${}^6\text{LiF}:\text{ZnS}(\text{Ag})$ → neutrons
- 50 Planes
 - 16x16 cubes
 - 64 wavelength shifting fibres
 - Fibres read out with SiPMs
- Detector
 - 5 modules of 10 planes each
 - Cooled to 5-10°C
- Goals
 - Measure neutrino oscillations at a 5-10m baseline
 - Measure ${}^{235}\text{U}$ anti-neutrino energy spectrum



Analysis

Atmospheric Background

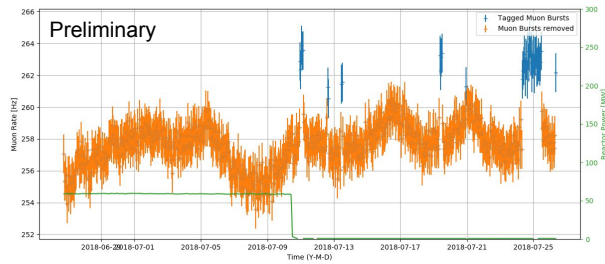
- Cosmic particles are the main source of background for reactor neutrino experiments with low overburden
 - The IBD selection ($S_{\text{Signal} - \text{BiPo}}$) is parametrized with the atmospheric pressure
 - Subtract reactor on from reactor off to get IBD excess
 - Define independent atmospheric selection (S_{atm})
 - Ratio between reactor on and off (χ_{atm}^S) gives atmospheric asymmetry for each reactor cycle
⇒ **excess is stable**
- Check the stability of the background with muon signals too



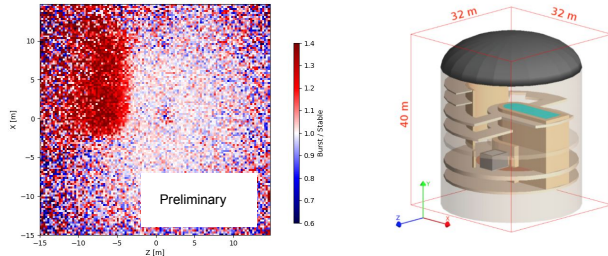
Stability

Muon Trending

- Muon rate variations due to changes in atmospheric conditions
 - Also sudden bursts are observed



- SoLid detector is perfectly fit for muon tomography
 - Bursts are due to drainage of reactor pool



Sensitivity to leptonic δ_{CP} with low energy atmospheric neutrinos and the effect of 1–2 oscillation parameters on δ_{CP} sensitivity at low energies

Lakshmi. S. Mohan¹, D. Indumathi^{2,3}, M. V. N. Murthy²

¹National Center for Nuclear Research, Poland

²The Institute of Mathematical Sciences, Chennai 600 113, India

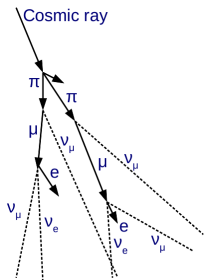
³Homi Bhabha National Institute, Mumbai, India

Lakshmi.Mohan@ncbj.gov.pl

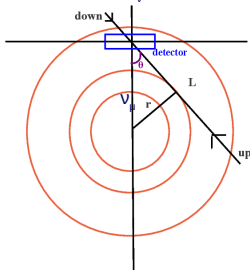
**40th International Conference on High Energy Physics, ICHEP
2020, Virtual conference**

31-07-2020

Hierarchy independent measurement of δ_{CP} with low energy atmospheric neutrinos [Phys. Rev. D **100** 11, 115027 (2019)]



Flux peaks at $E_\nu < 1$ GeV



Span a wide range of L/E_ν

Oscillation probability of $\nu_\alpha \rightarrow \nu_\beta$ in vacuum

$$P_{\alpha\beta}^{(-)vac} = \delta_{\alpha\beta} - 4 \sum_{i>j} \text{Re} [U_{\alpha i} U_{\beta i}^* U_{\alpha j}^* U_{\beta j}] \sin^2 \left(\frac{1.27 |\Delta m_{ij}^2| L}{E} \right) \pm 2 \sum_{i>j} \text{Im} [U_{\alpha i} U_{\beta i}^* U_{\alpha j}^* U_{\beta j}] \sin \left(\frac{2.53 \Delta m_{ij}^2 L}{E} \right).$$

$$U_{\alpha i}^{vac} = \begin{pmatrix} c_{12}c_{13} & s_{12}c_{13} & s_{13}e^{-i\delta} \\ -c_{23}s_{12} - s_{23}c_{12}s_{13}e^{i\delta} & c_{23}c_{12} - s_{23}s_{12}s_{13}e^{i\delta} & s_{23}c_{13} \\ s_{23}s_{12} - c_{23}c_{12}s_{13}e^{i\delta} & -s_{23}c_{12} - c_{23}s_{12}s_{13}e^{i\delta} & c_{23}c_{13} \end{pmatrix}$$

where $c_{ij} = \cos \theta_{ij}$ and $s_{ij} = \sin \theta_{ij}$; $i, j \rightarrow$ mass eigenstates.
 $\theta_{ij} \rightarrow$ mixing angles; $\delta_{cp} =$ leptonic CP violation phase

For $E \sim$ a few 100 MeV, the corresponding oscillatory terms average out when $L/E \gg \Delta m_{ij}^2$

- For “atmospheric” terms \rightarrow rapid oscillations and averaging out :

$$1.27 \Delta m_{3j}^2 L/E \approx \pi \frac{(L/100 \text{ km})}{(E/0.1 \text{ GeV})}, \quad (1)$$

The event rates at these low energies and $L \gtrsim$ few 100 km are independent of Δm_{32}^2 and Δm_{31}^2 and hence of their ordering.

δ_{CP} sensitivity from sub-GeV charged current electron like events –

Realistic case

Probabilities of interest:

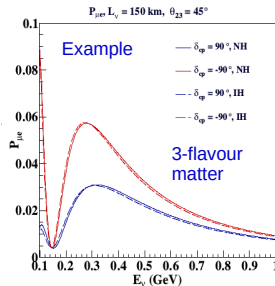
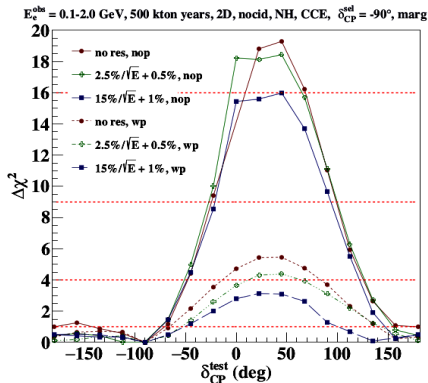
$$P_{ee}, P_{\mu e}, \bar{P}_{ee}, \bar{P}_{\mu e} \text{ and } P_{e\mu}, P_{\mu\mu}, \bar{P}_{e\mu}, \bar{P}_{\mu\mu}$$

$E_l^{obs}, \cos \theta_l^{obs}$ - 2D binning:

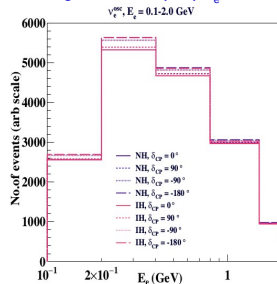
$$\chi^2 = \sum_{i=1}^{N_{E_l^{obs}}} \sum_{j=1}^{N_{\cos \theta_l^{obs}}} 2 \left[(T_{ij} - D_{ij}) - D_{ij} \ln \left(\frac{T_{ij}}{D_{ij}} \right) \right] + \sum_{l=1}^3 \xi_l^2$$

Systematic uncertainties - 5% each in “tilt”, flux normalisation and cross section

50 kTon isoscalar detector X 10 years of exposure = 500 kton years



Charged current (CC) ν_e events



Sensitivity to 1–2 parameters and their effect on δ_{CP} sensitivity from sub-GeV CCE events [Preliminary]

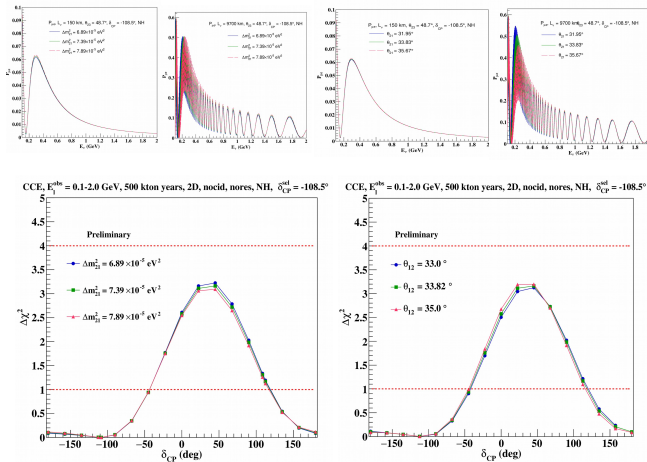


Figure 1: No sensitivity to 1–2 parameters themselves and 1–2 parameters have no effect on δ_{CP} sensitivity from sub-GeV atmospheric CCE events.



Production of ^{83}Rb for calibration sources for dark matter and neutrino mass experiments

M. Šefčík, D. Vénos, R. Běhal, O. Dragoun, O. Lebeda, D. Seifert, J. Ráliš

Nuclear Physics Institute, Czech Academy of Sciences

250 68 Řež, Czech Republic

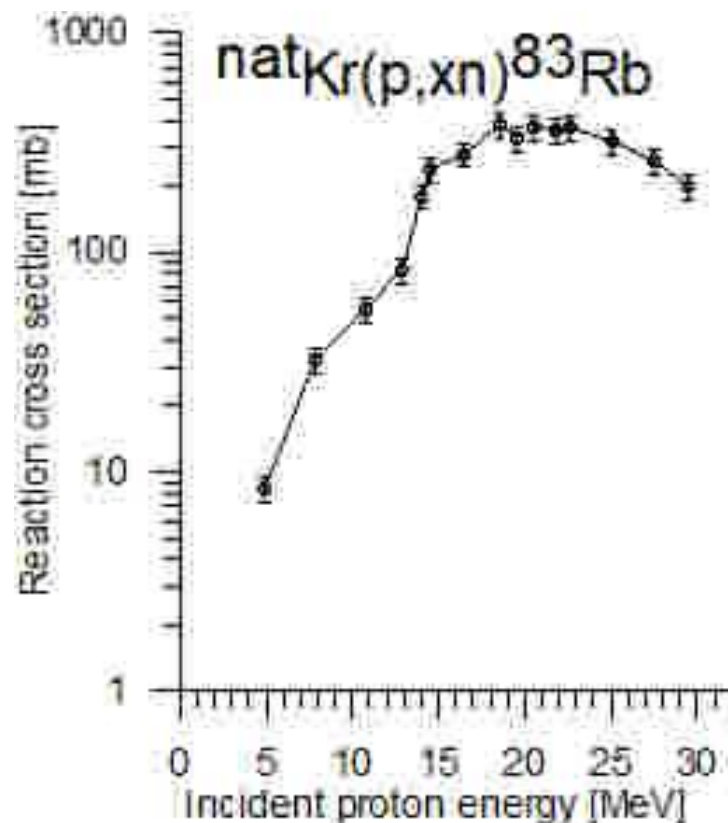


Motivation

- Decays:
 - ^{83}Rb ($T_{1/2} = 86.2 \text{ d}$) \rightarrow $^{83\text{m}}\text{Kr}$
 - $^{83\text{m}}\text{Kr}$ ($T_{1/2} = 1.8 \text{ h}$) \rightarrow ^{83}Kr
- **Monoenergetic electrons** of internal conversion of $^{83\text{m}}\text{Kr}$ have a well known low energy.
- They are suitable for **the test, calibration and systematic measurements** of detector systems.
- Examples of use:
 - At KATRIN:
 - To investigate the properties of **the windowless gaseous tritium source** and high-energy-resolution **electrostatic electron spectrometers**.
 - To calibrate the measurements of the **high voltage** and monitor its stability.
 - At XENON, for calibration of the energy scale of **the xenon liquid detector**.
 - At ALICE (CERN), for calibration of **the Transition Radiation Detector**.

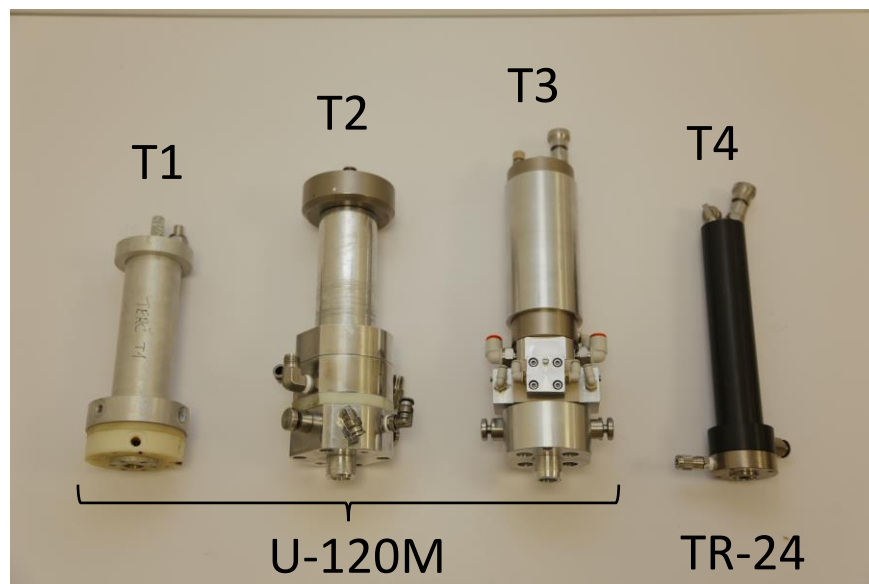
^{83}Rb production

- Isotope ^{83}Rb is produced in the **reaction of protons on the natural krypton gas**.
- The main contributing reaction is $^{84}\text{Kr}(p,2n)^{83}\text{Rb}$.
- Smaller amounts of radioactive isotopes ^{84}Rb ($T_{1/2} = 33$ d) and ^{86}Rb ($T_{1/2} = 19$ d) are **also produced** in the reaction.
- They **do not disturb the $^{83\text{m}}\text{Kr}$ in its applications** because the intensity of their low energy electrons is weak.
- For the irradiation of natural krypton with protons at the NPI cyclotrons a **pressurised gas target is used**.



Production method development

- For the **cyclotron U-120M** ($E_p=26.5$ MeV, $I_p=15$ μ A) and the new **cyclotron TR-24** ($E_p=24$ MeV, $I_{pmax}=45$ μ A), gradually four types of the targets (from T1 to T4) from the aluminium alloy were developed and used.
- Up to now the most efficient **target T4** is irradiated with a proton current 45 μ A, with initial krypton pressure of 10 bar. The **^{83}Rb production rate is 150 MBq/hour**.
- Further steps for production **optimization**:
 - **Target length** - to reduce ^{84}Rb and ^{86}Rb production.
 - Alloy with **less Fe and Ni** - to **decrease the contamination** with radioactive Co isotopes.
 - Try to **irradiate at 25 MeV** at TR-24 (needs a special cyclotron regime) - to reduce ^{84}Rb and ^{86}Rb production.
 - **Larger defocusing** of the proton beam at the target input windows **to reduce their local thermal load**.



Antineutrinos from the Sun and Sterile Neutrino Decays



ICHEP 2020 | PRAGUE

from $p^2 = m^2$ to $p^2 \neq m^2$

Matheus Hostert

University of Minnesota & Perimeter Institute



UNIVERSITY OF MINNESOTA

in collaboration w/ Maxim Pospelov
to appear

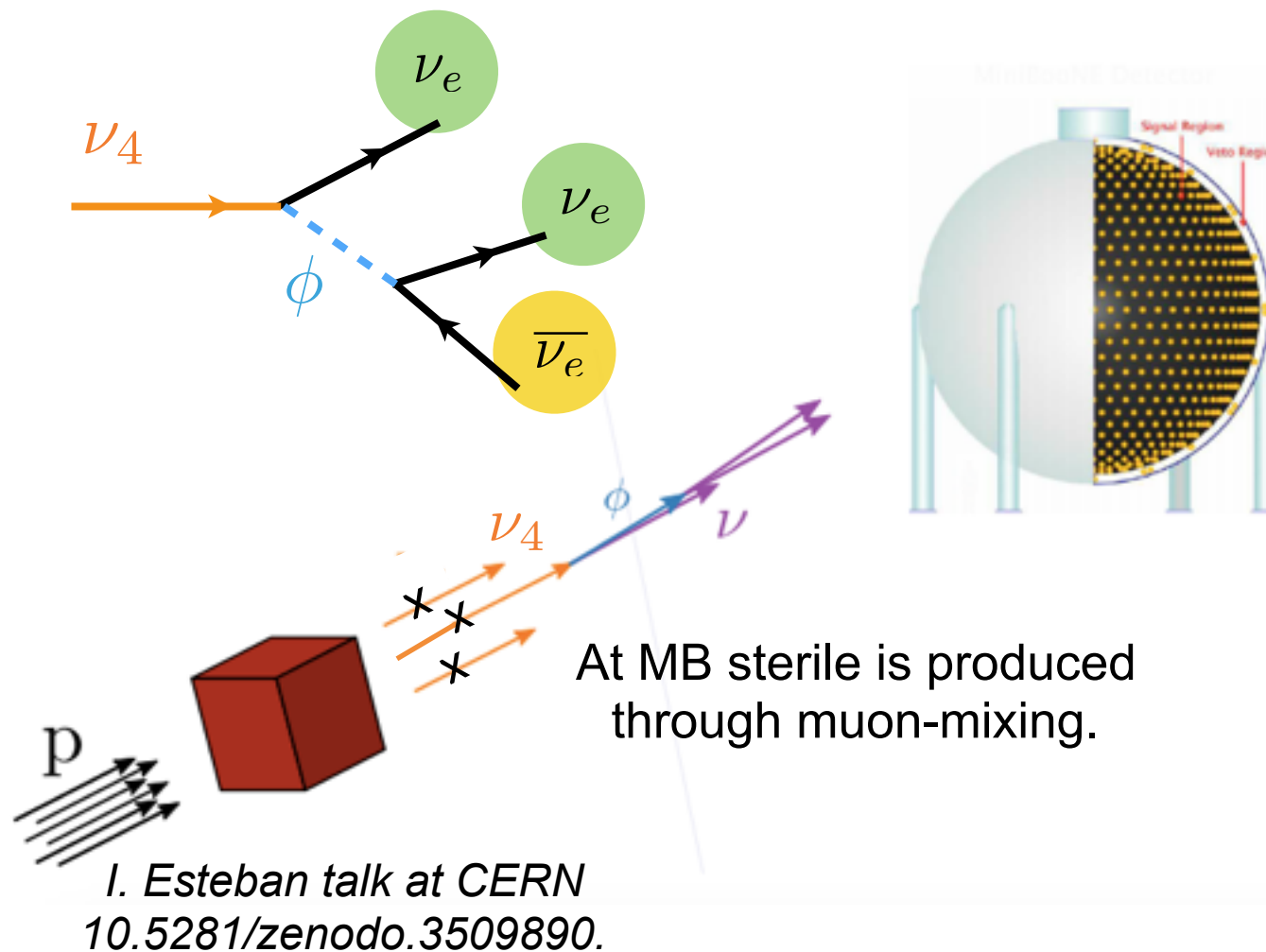


A shift from eV sterile neutrinos to explain SBL anomalies

Sterile neutrino visible decays:

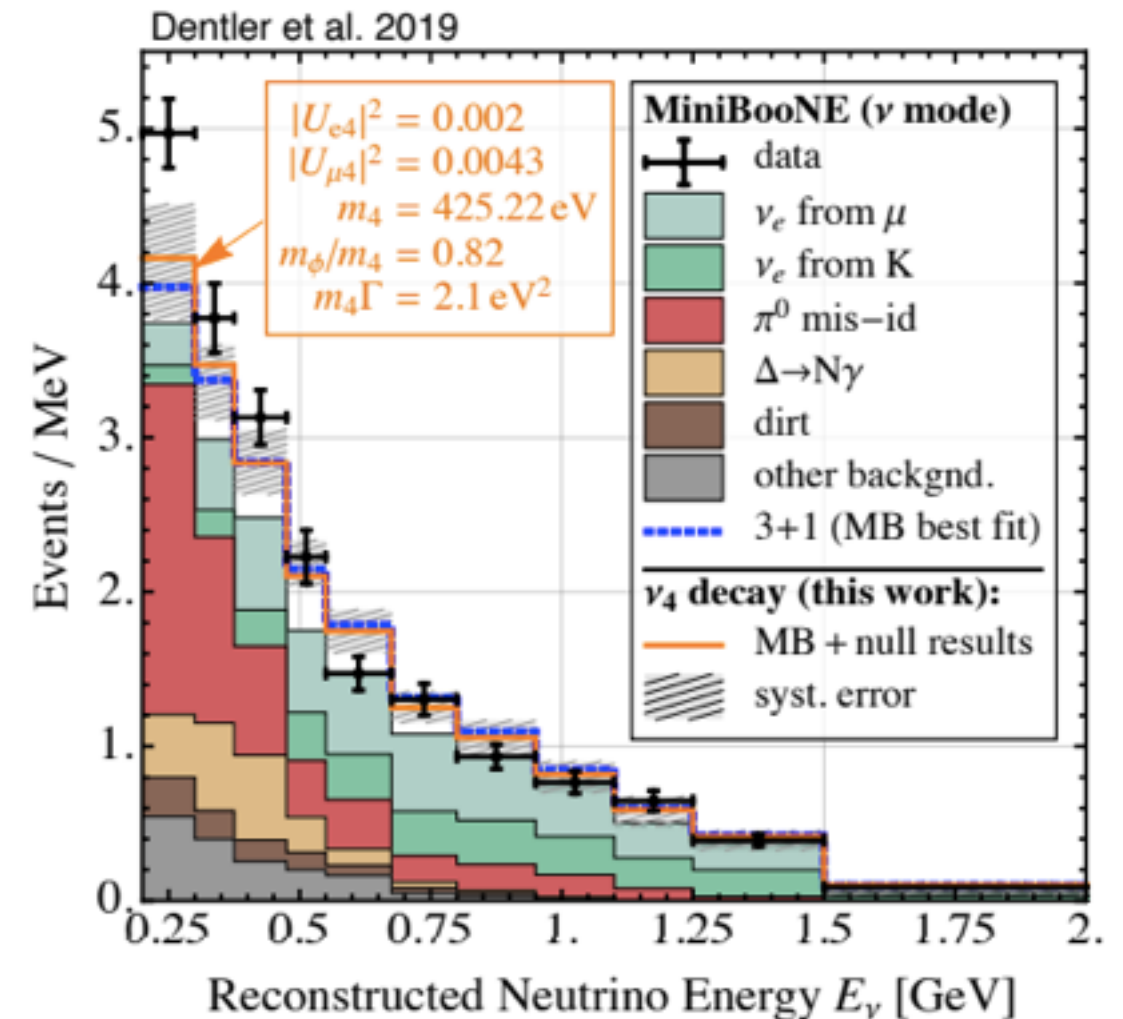
M. Dentler *et al*, *PRD101*(2020) 115013.

$$-\mathcal{L} \supset g_s \bar{\nu}_s \nu_s \phi + m_{ab} \bar{\nu}_a \nu_b.$$



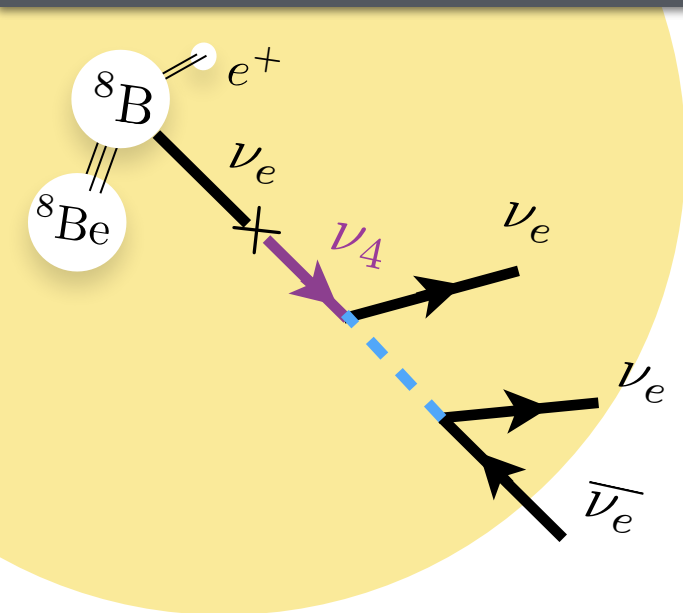
An effective $\nu \rightarrow \bar{\nu}$ transition

MiniBooNE energy distribution



Avoids tension with disappearance exps,
and may be extended to satisfy cosmology.

Existing constraints on Solar antineutrinos



$\bar{\nu}_e$ detection through
Inverse Beta Decay

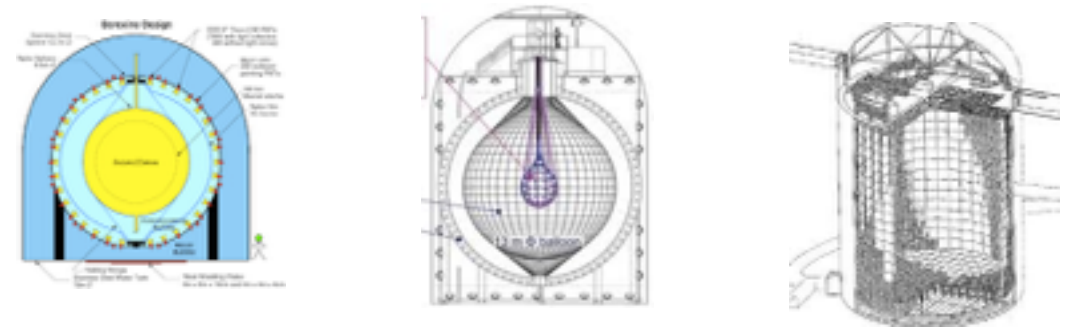
$$\bar{\nu}_e + p^+ \rightarrow e^+ + n$$

IBD has **small backgrounds** and much **larger cross section** than nu-e elastic!

$$\sigma_{\text{IBD}} \gg \sigma_{\nu-e}$$

When produced, $\bar{\nu}_e$ undergoes **matter-suppressed** flavour transitions.

The Sun does not emit antineutrinos:



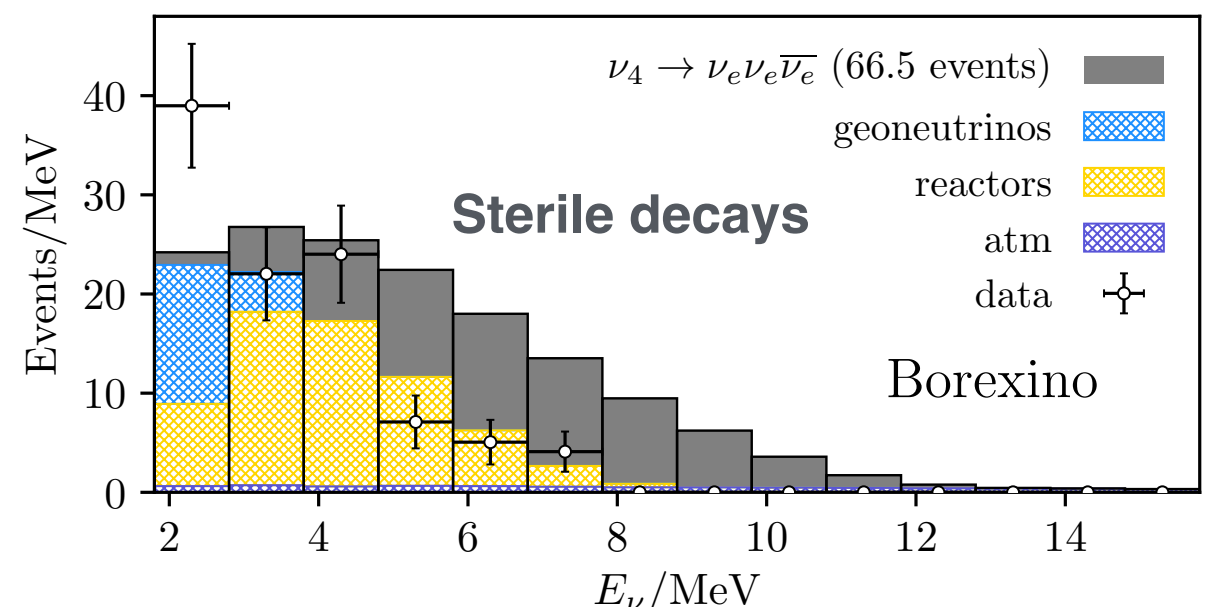
$$P_{\nu_e \rightarrow \bar{\nu}_e}^{\text{Borexino}}(E_\nu \geq 1.8 \text{ MeV}) < 7.2 \times 10^{-5}$$

$$P_{\nu_e \rightarrow \bar{\nu}_e}^{\text{KamLAND}}(E_\nu \geq 8.3 \text{ MeV}) < 5.3 \times 10^{-5}$$

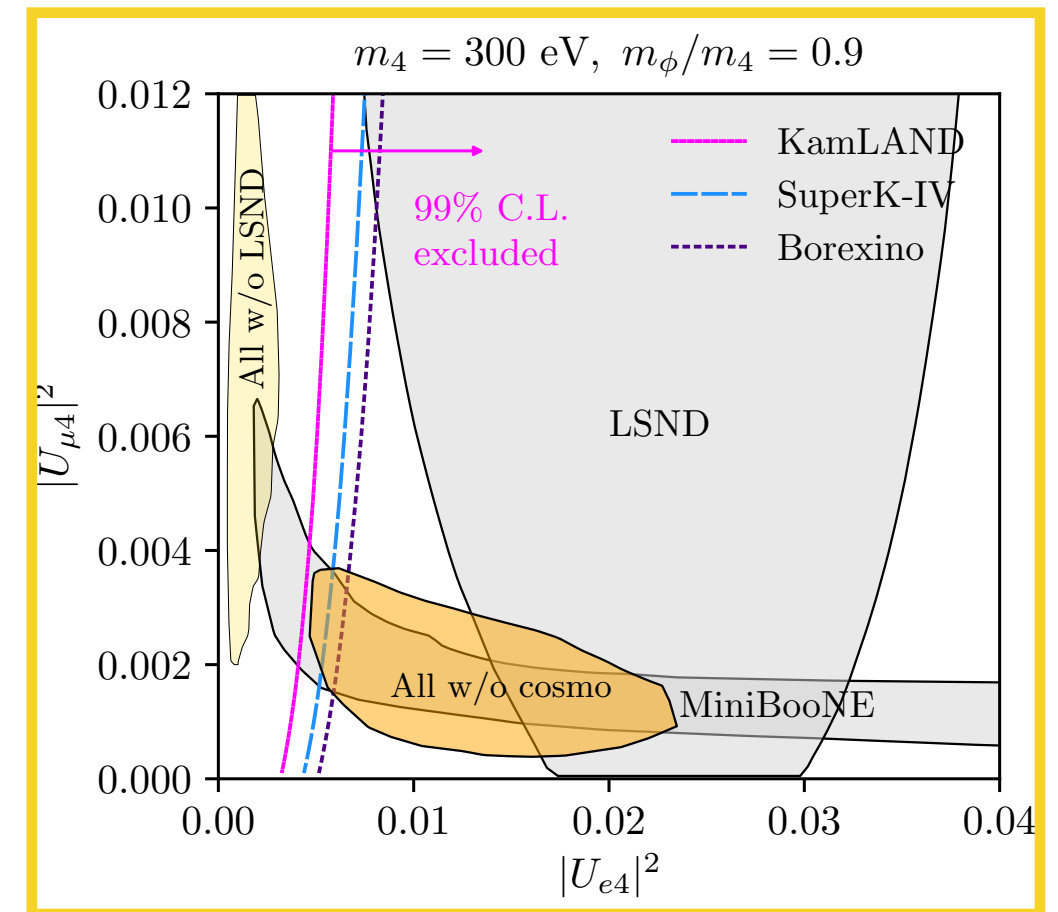
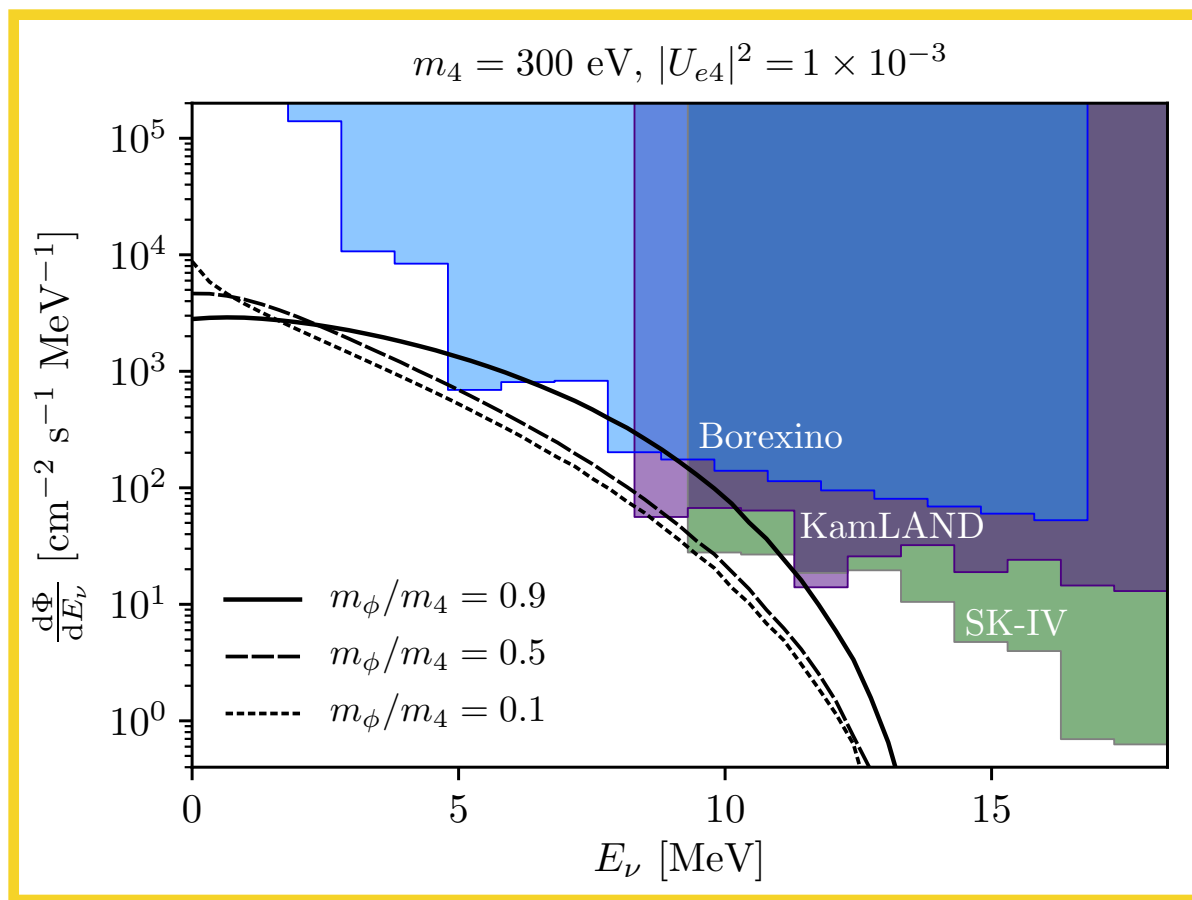
$$*P_{\nu_e \rightarrow \bar{\nu}_e}^{\text{SK-IV}}(E_\nu \geq 9.3 \text{ MeV}) \lesssim 1.0 \times 10^{-4}$$

From a dedicated simulation of the NP signature:

$$m_4 = 300 \text{ eV}, m_\phi/m_4 = 0.90, |U_{e4}|^2 = 5 \times 10^{-3}$$



Predictions of decaying-sterile hypothesis



A simultaneous explanation of LSND and MiniBooNE is in tension with Solar antineutrino searches.

Significant improvement expected at JUNO and SK-Gd

S.J. Li *et al*, *Nucl.Phys.B* 944(2019)114661

Bounds becomes stronger for Majorana neutrinos, but may be weakened if:

- Only MiniBooNE is explained and taking small m_ϕ/m_4

- Complicate the model and decouple decay from

electron-heavy mixing: S. Palomares-Ruiz *et al*, *JHEP*09(2005)048

A. deGouvea *et al*, *JHEP*07(2020)141

Fast Neutrino Flavor Conversion At Late Time

Soumya Bhattacharyya¹

soumyaquanta@gmail.com

Jul 31, 2020



ICHEP 2020 | PRAGUE

¹Department of Theoretical Physics, TIFR

Background

- High neutrino density inside supernovae allows self-interaction of strength, $\mu \gg \lambda$ (matter potential), ω (vacuum scale)
- Such conditions favor fast flavor conversion : 1) *Rapid and occurs at a rate μ* 2) *Can give rise to complete flavor conversion* 3) *System gets coupled and also nonlinear*
- Linear stability analysis done in previous literatures helps to understand if or when FFC occurs but fails to study the impact of FFC on the observable neutrino fluxes or explosion mechanism

PhysRevD.84.053013 (2011)

Motivation

- Understanding the nonlinear mechanism of fast conversions both numerically and analytically considering a system of *inhomogeneous and non-stationary dense neutrino gas* with *1 (space) +1 (momentum)+1 (time) phase space dimensionality*

Equations Of Motion

$$\left(\partial_t + v \partial_x \right) \mathbf{P}_v(x, t) = \mu \underbrace{\left(\mathbf{M}_0(x, t) - v \mathbf{M}_1(x, t) \right)}_{\mathbf{H}_v} \times \mathbf{P}_v(x, t)$$

$$\mathbf{M}_n = \int_{-1}^1 L_n(v) \mathbf{P}_v dv$$

JCAP 03, 042 (2016)

JCAP 02, 019 (2017)

Numerical Strategy

- Discretize in space for every v
- Solve a set of coupled nonlinear O.D.E in t
- Method : B.D.F Boundary Condition : Periodic in space
- Solver : Zvode and scipy.fftpack.diff in python

1) Pendulum Motion

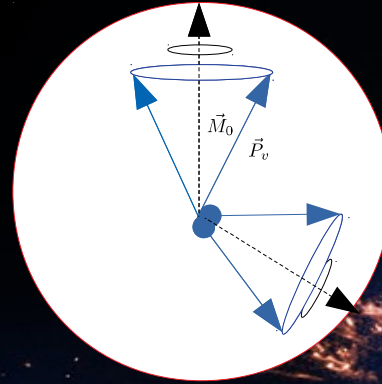
Results

2) Non-separable solution in x & v

- Stationarity in time
- Each P_v shows a precession around M_0 in space
- M_0 shows pendulum motion in space

Phys. Rev.D 74, 105010 (2006)

Phys. Rev. D 101,043009 (2020)



- Stationary solution for every P_v is non-separable in x & v for any lepton asymmetry (A)
- This can be checked through the spatial dependence of the quantity,

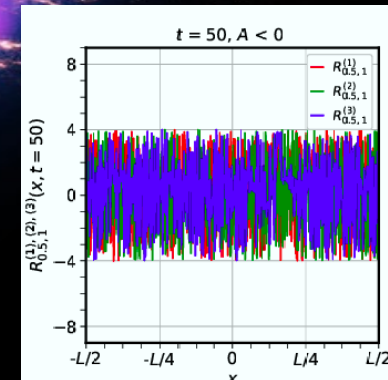
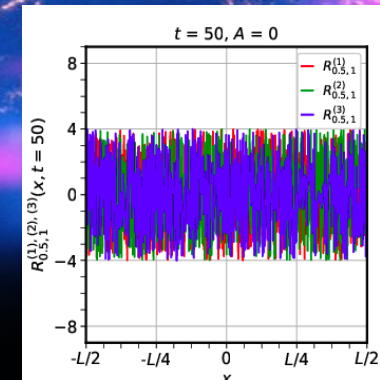
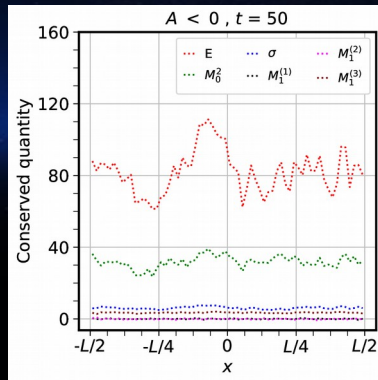
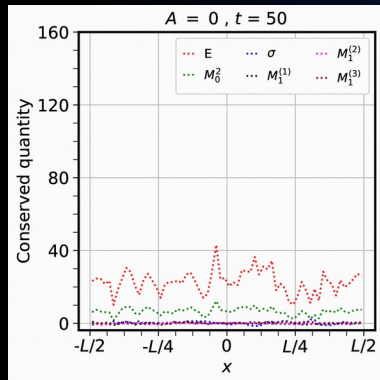
$$R_{v_1, v_2}^i(x) = \frac{P_{v_1}^i(x)}{P_{v_2}^i(x)} \Big|_{t=50} \quad i = 1, 2, 3$$

$$\tilde{\mathbf{P}}_v : \frac{d}{dx} \tilde{\mathbf{P}}_v(x) = \frac{\tilde{\mathbf{M}}_0(x)}{v} \times \tilde{\mathbf{P}}_v(x)$$

$$\tilde{\mathbf{M}}_0 : \tilde{\mathbf{M}}_0 \times \frac{d^2}{dx^2} \tilde{\mathbf{M}}_0 + \sigma \left| \tilde{\mathbf{M}}_0 \right| \frac{d}{dx} \tilde{\mathbf{M}}_0 = \left| \tilde{\mathbf{M}}_0 \right|^2 \tilde{\mathbf{B}} \times \tilde{\mathbf{M}}_0$$

$$E = \tilde{\mathbf{B}} \cdot \tilde{\mathbf{M}}_0 + \frac{1}{2} \tilde{\mathbf{D}} \cdot \tilde{\mathbf{D}} \quad \sigma = \tilde{\mathbf{D}} \cdot \tilde{\mathbf{M}}_0 \quad \left| \tilde{\mathbf{M}}_0 \right| = \text{const}$$

$$\tilde{\mathbf{D}} = \sum_{n=\text{odd}} \alpha_n \tilde{\mathbf{M}}_n, \quad \tilde{\mathbf{B}} = \sum_{n=\text{even}} \beta_n \tilde{\mathbf{M}}_n$$



Results

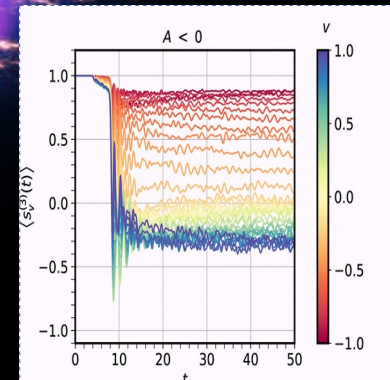
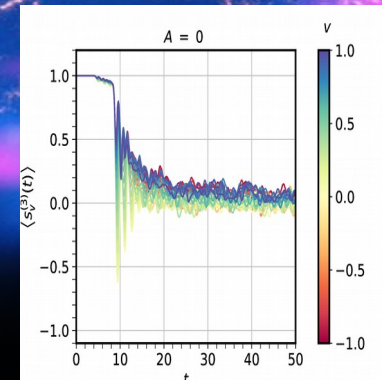
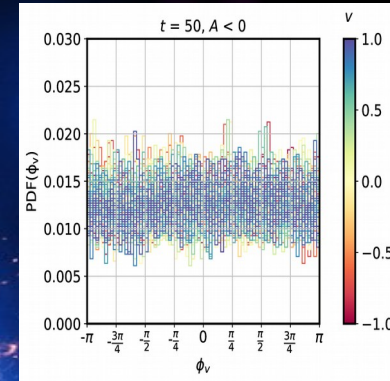
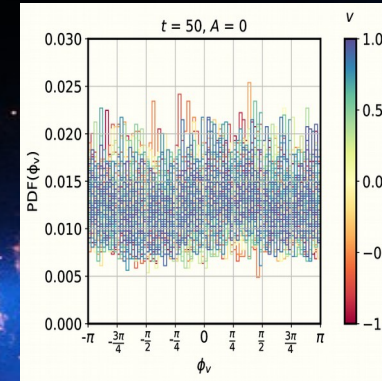
3) Phase Randomization

- The phase between the transverse components of P_v gets completely random between $[-\pi, \pi]$ in space independent of any value of v and A at late times.

arXiv: 2005.00459

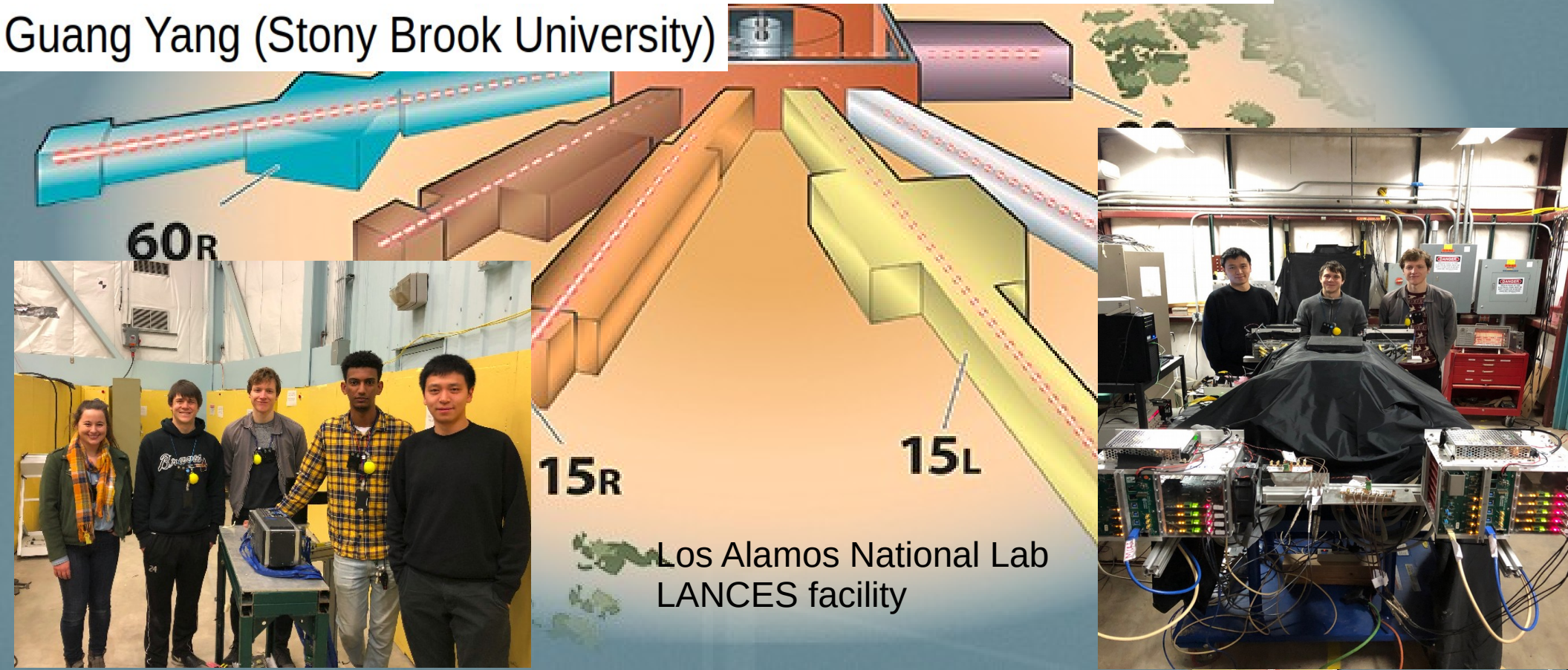
4) Depolarization in velocity space

- The spatially averaged P_v exhibit complete (or partial) decoherence for zero (or nonzero) lepton asymmetry at late times. [Phys. Rev. D 75, 083002 \(2007\)](#) [Phys. Rev. D 76, 125018 \(2007\)](#)
- For partial decoherence the vanishing range of velocity modes loosely depends on the occurrence of the sign-flip of the z component of the Hamiltonian in corotating frame
- This kinematic decoherence stems from randomization of the transverse components of P_v



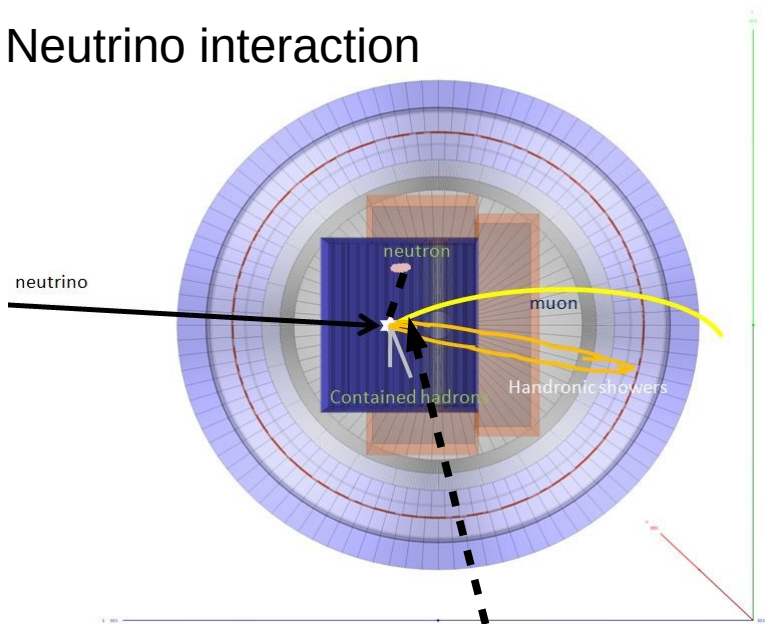
Neutron Beam Test with 3D-Projection Scintillator Tracker Prototypes for Long-Baseline Neutrino Oscillation Experiments

Guang Yang (Stony Brook University)



Motivation

Neutrino interaction



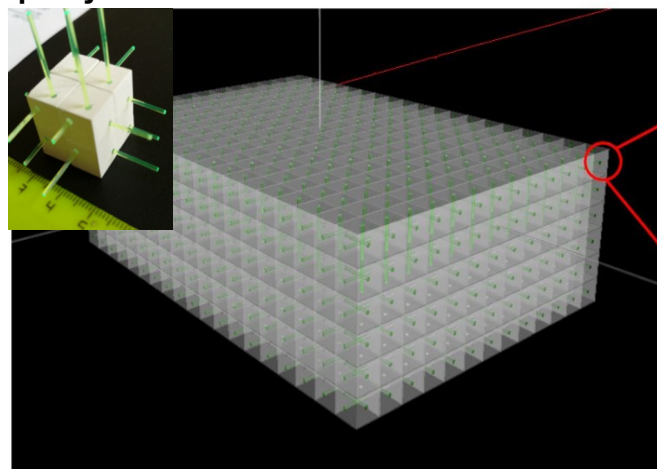
- Neutron kinetic energy can be obtained by measuring the neutron-induced hit distance and time

- Missing neutron energy : one of the dominant systematic uncertainties in the long-baseline neutrino oscillation analyses

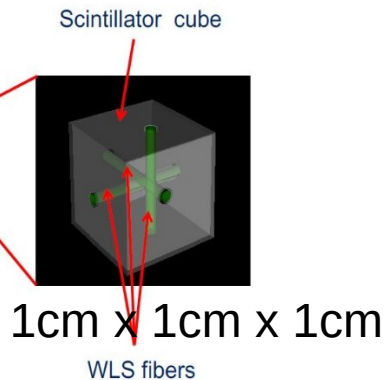
- In the precision era, neutrino interaction measurement including neutron information desired in the near detectors of the long-baseline experiments

- Neutron kinetic energy measurement enabled by the ToF technique with a low-threshold, fast-timing and fine-granularity 3D projection tracker

3D projection scintillator tracker



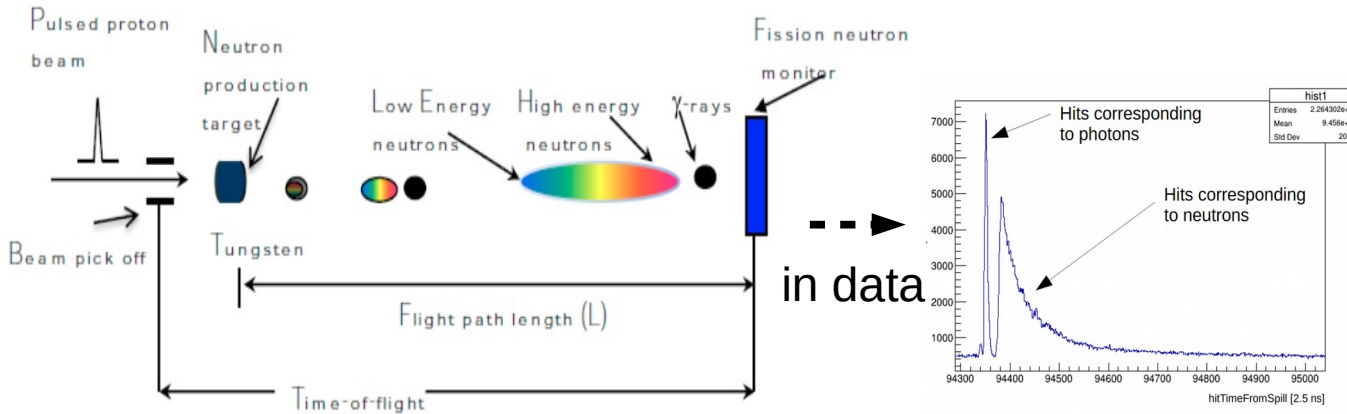
3 fiber light yield: > 100 pe
MIP time resolution ~ 0.5 ns



Beamline setup



Stony Brook University



Collaborating institutions

- CERN
- University of Geneva, Switzerland
- High Energy Accelerator Research Organization (KEK), Japan
- Institute for Nuclear Research (INR), Russia
- Imperial College, UK
- Louisiana State University, USA
- University of Pennsylvania, USA
- University of Pittsburgh, USA
- University of Rochester, USA
- Stony Brook University, USA
- University of Tokyo, Japan
- ETH Zurich, Switzerland
- Chung-Ang University, S. Korea
- South Dakota School of Mines and Technology, USA
- A lot thanks to the LANSCE's WNR facility

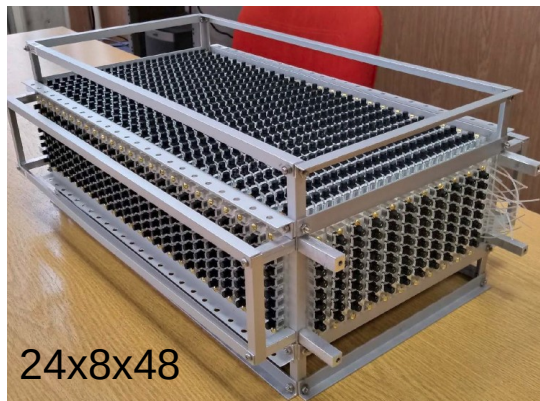
- We have two separate beamline time allocations at 90 m and 20 m locations from the proton target.
- A gamma flash (providing t_0) comes before the neutron arrives, which allows a neutron energy measurement with the time-of-flight.
- Two prototypes were proposed and built by a collaboration and exposed to the beamline for a total time of 90 hours.

LANSCCE neutron beam test



Stony Brook University

SuperFGD prototype

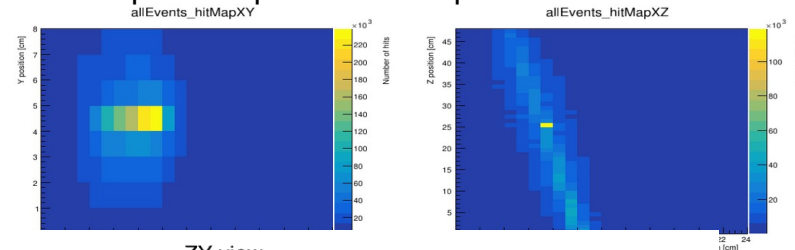


US-Japan prototype

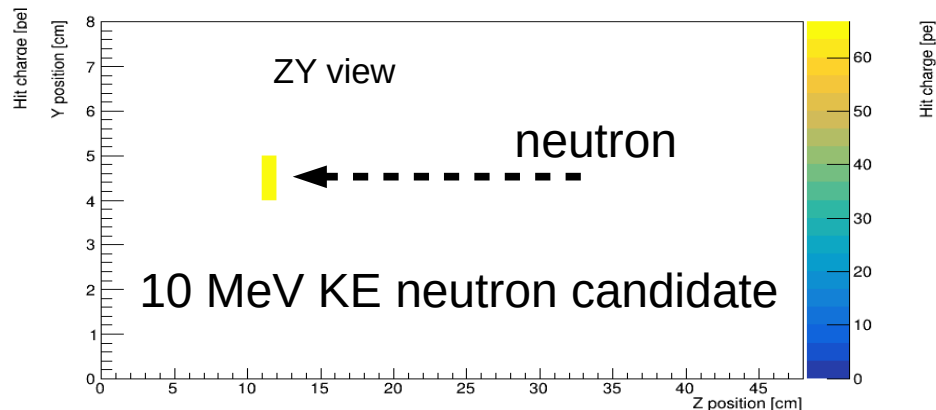
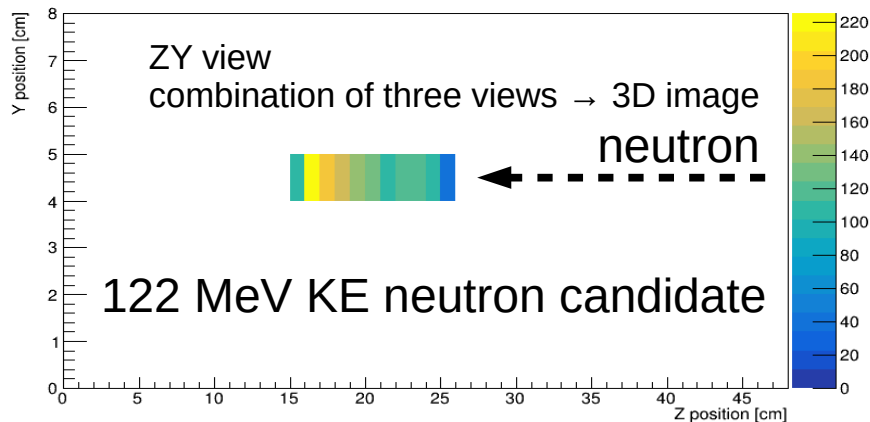


- A ~0-800 MeV KE neutron beam provided by LANSCE in LANL; Our detectors capable to achieve an energy resolution measurement at 2% level
- Goals: Neutron detection response, neutron cross section and neutron double scattering; Data analysis is on-going and we expect a publication by the end of this year.

SuperFGD proto. Beam spot XY and XZ



ZY view



SuperNEMO Calorimeter Commissioning

Malak HOBALLAH on behalf of the SuperNEMO Collaboration
Jul 31 2020

ICHEP 2020 | PRAGUE

40th INTERNATIONAL CONFERENCE
ON HIGH ENERGY PHYSICS

**VIRTUAL
CONFERENCE**

28 JULY - 6 AUGUST 2020

PRAGUE, CZECH REPUBLIC



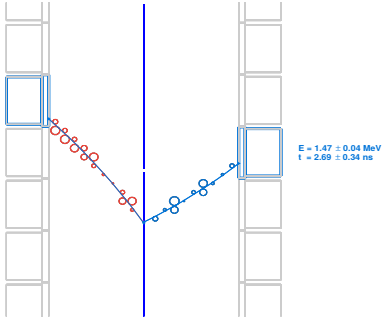
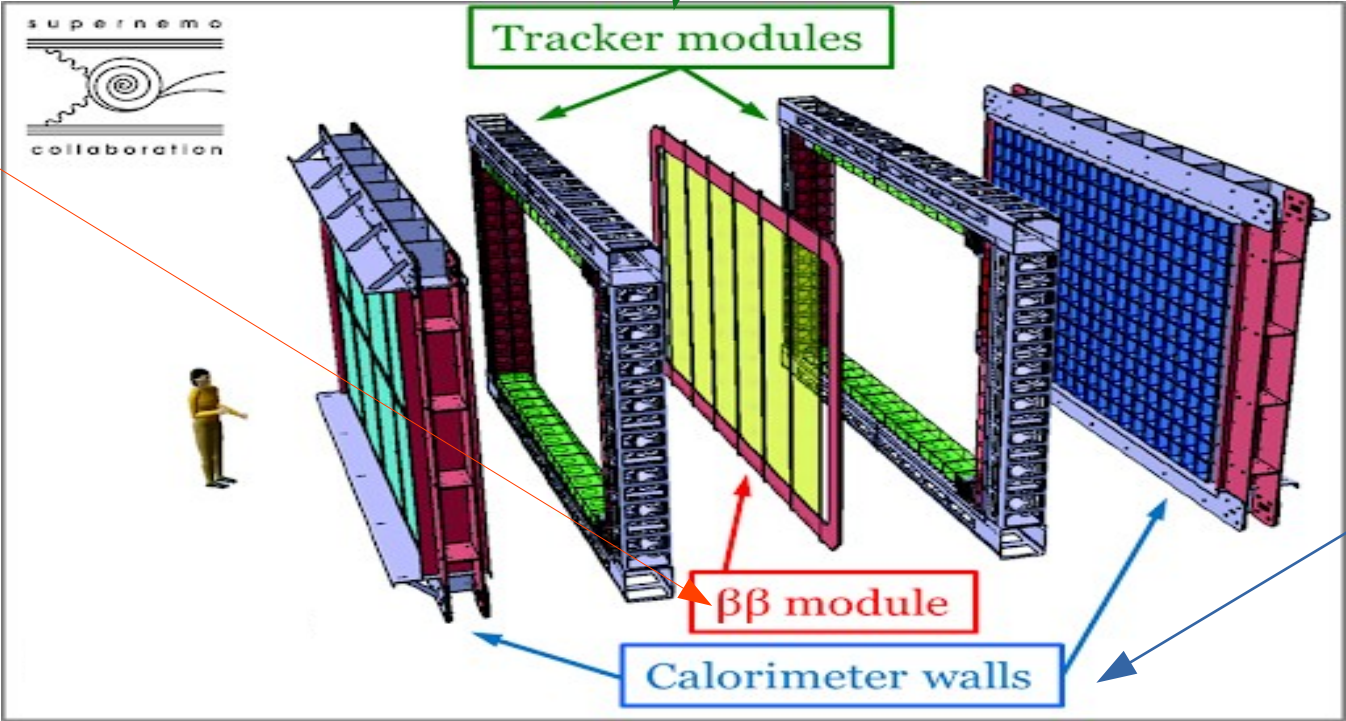
université
PARIS-SACLAY



SuperNEMO and Neutrinoless Double Beta Decay ($0\nu\beta\beta$)

Full topological reconstruction → **High background rejection**
(expected $<10^{-4}$ events/keV/kg.yr)

Source separate
from detector
→ ability to **study
several isotopes**



Measure individual
energies giving access
To decay mechanism

Main goal to reach a sensitivity of $T_{1/2}^{0\nu} > 5 \cdot 10^{26}$ y with 500 kg.y exposure of ^{82}Se

The SuperNEMO Demonstrator & Calorimeter

Demonstrator module with ~ 6 kg of ^{82}Se :

Expected sensitivity $T_{1/2}^{0\nu} > 6.5 * 10^{24} \text{ y}$, $\langle m_{\nu} \rangle < (0.15 - 0.4) \text{ eV}$ (90% CL) for a 17.5 kg.y exposure of ^{82}Se

Reachable background sensitivity Source radio-purity $A(^{208}\text{Tl}) < 2 \mu\text{Bq/kg}$ & $A(^{214}\text{Bi}) < 10 \mu\text{Bq/kg}$ $A(^{222}\text{Rn}) < 0.15 \text{ mBq/m}^3$

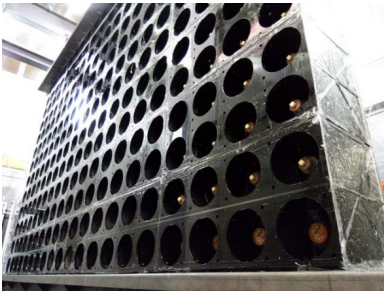
The Calorimeter of the Demonstrator :



Specifications

Energy resolution
8% FWHM at 1 MeV

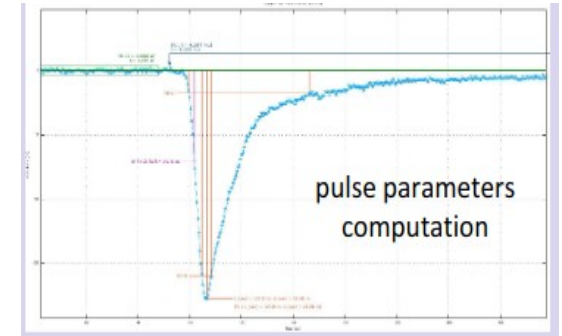
Time resolution $\sigma < 400 \text{ ps}$
for 1 MeV electrons



712 optical modules

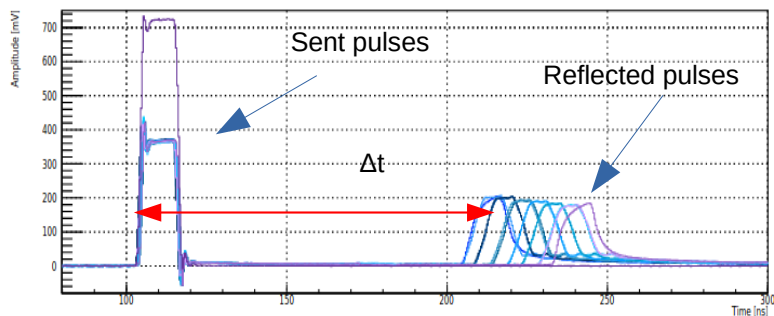


Pulse digitization:
pedestal and pulse
shape tested using
background runs

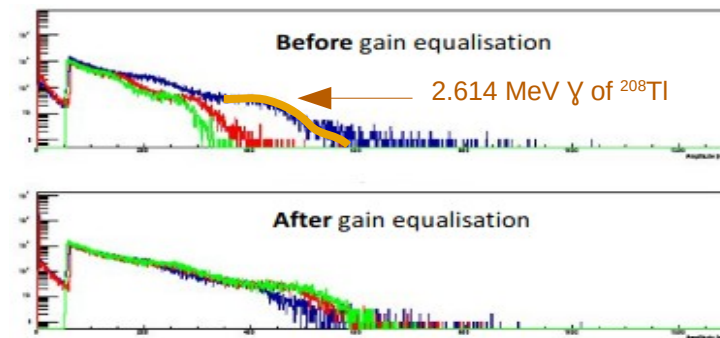


Tracker on its final steps towards commissioning, magnetic field, anti-Radon tent, gamma and neutron shielding to be installed

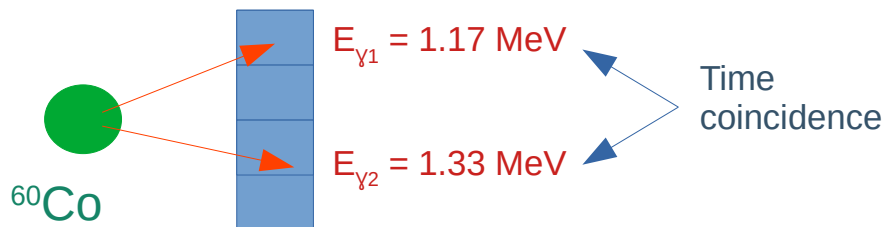
Calorimeter Commissioning analysis



Reflectometry tests to test signal attenuation and time delays between PMT channels using electronics generated pulses



PMT Gain equalization with a dedicated method using ^{208}Tl Compton edge, giving a spread in gain $< 10\%$ with gammas, better results expected with electrons



Time resolution primarily results using ^{60}Co give a $\sigma < 600 \text{ ps}$ for γ s @ 1 MeV

Better results expected with an electron source and tracker commissioned

**Thanks for your
attention**